ELSEVIER

Journal of Nuclear Materials 301 (2002) 210–219

journal of nuclear materials

www.elsevier.com/locate/jnucmat

Kinetic theory of the growth of the circular oxidation islands on the UO_2 surface

Miroslav Kolář *

AECL, Whiteshell Laboratories, Pinawa, MB, Canada R0E 1L0

Received 11 January 2001; accepted 15 October 2001

Abstract

Island-like oxidation of a solid surface is studied. Such a process occurs for example at the beginning of the second stage of the oxidation of UO_2 to U_3O_8, and its study is thus important for handling of used nuclear fuel in intermediate dry air storage. Mathematical formulation of the problem is presented, approximate analytical formulas are derived and discussed for the isothermal case, and the non-isothermal case is studied numerically. It is shown that for the accurate prediction of the UO_2 surface oxidation, it is important to know separately the rates of island nucleation and of island-radius growth. Only a certain product of these two rates can be obtained from isothermal experiments. Here we show how one can determine directly the values of the activation energies of both these rates from a series of suitably designed accelerated non-isothermal experiments.

PACS: 28.41.Kw; 82.65.−i; 28.41.Te; 28.41.Bm

1. Introduction

For spent nuclear fuel placed in intermediate dry air storage, it is very important to know with high accuracy the rates associated with the second stage of the UO_2 oxidation. This stage is characterized by the creation of U_3O_8, which is accompanied by a considerable increase of the specific volume of the oxide. This volume increase can cause the splitting of the sheath of a spent nuclear fuel element with a tiny defect enabling ingress of oxygen and thus oxidation, which could result in the release of active U_3O_8 powder into the storage container. This would complicate considerably the subsequent handling and permanent disposal of the fuel.

The oxidation of a UO_2 surface is generally a two stage process [1]. In the first stage the surface is covered at low temperatures by a continuous layer oxidized to about U_3O_7 (unirradiated UO_2) or to U_4O_{9+x} (e.g., LWR spent fuel). The second stage (which may proceed at different speeds in unirradiated UO_2 and in various spent fuels) consists of nucleation and subsequent growth of U_3O_8 islands. This paper deals with the second stage only, namely with the initial phase of the second stage characterized by less than 50% of the total surface covered with U_3O_8. The reader is referred to a previous paper [1] on the island-like oxidation, and to the references cited therein, for a detailed discussion of the underlying chemical processes and the justification of the model used. Here the emphasis is on the mathematical aspects of the model.

The previous paper [1] dealt in a considerable detail with the isothermal case, in particular with the determination of an activation energy for the formation of U_3O_8 on the surface of UO_2. This activation energy is a combination of the activation energies of the two subprocesses, which cannot be separated in an isothermal experiment. However, the knowledge of the individual values of these two partial activation energies is necessary e.g. for the accurate prediction of the used fuel behavior in a dry air storage. The present paper

* Tel.: +1-204 753 2311, x2498; fax: +1-204 753 2690.
E-mail address: kolarm@aecl.ca (M. Kolář).

0022-3115/02/$ - see front matter
PII: S0022-3115(01)00740-1

therefore goes beyond the isothermal case, and shows how the values of the two partial activation energies can be obtained from non-isothermal experiments.

In Section 2, kinetic equations (a set of three simple first-order ordinary differential equations) describing the nucleation and growth of the circular oxidation islands for general (temperature and therefore time dependent) rates of island nucleation and growth are derived. Then, in Section 3, the previous discussion [1] of the isothermal case is completed by adding a few more details on the accuracy of the truncated Taylor-series approximations. From a series of isothermal experiments one can only determine a convoluted 'lumped' rate constant and its activation energy (of the U_3O_8 formation mentioned above). This lumped rate is a certain product of the two individual rates of island nucleation and growth. Finally, in Section 4, numerical solutions of the general kinetic equations are obtained for different temperature scenarios using different decomposition of the lumped activation energy into the two partial ones. The sensitivity of the degree of surface oxidation to the variation of the values of these two activation energies is found to be significant. It is thus desirable to determine the values of both activation energies separately. The last part of Section 4 shows how a series of suitably designed non-isothermal experiments may achieve this. Section 5 then summarizes the new results and draws conclusions for possible experimental work.

2. Formulation of the problem

In the previous paper [1], detailed derivation of the kinetic equation governing the time dependence of the fraction of the surface covered by the oxidation islands can be found for the case of constant rates of nucleation and of island growth. Following the same line of reasoning, here we derive a more general expression. The two-dimensional model used in this approach is deemed appropriate because comparison is made with X-ray diffraction data with a sampling depth of less than 1 μm.

Let us assume that we have a flat surface of area F that is subjected to the island type of oxidation. The rate at which the microscopic nuclei of new islands per unit area of the free (still uncovered) surface are formed at time t is $K_n(t)$. The dependence of $K_n(t)$ on time t is implicit: K_n is a function of the surface temperature, and the surface temperature can vary with time in an arbitrary way.

Assuming that the growth of each island is isotropic, we can introduce a single linear rate of growth, $K_g(t)$, of the radii of all islands at time t. K_g again depends implicitly on time through possible temperature variation with time.

Both rates are assumed to have the Arrhenius dependence on temperature,

$$K_n(T) = c_n \mathrm{e}^{-E_n/RT}, \tag{1}$$

and

$$K_g(T) = c_g \mathrm{e}^{-E_g/RT}, \tag{2}$$

where T is the absolute temperature (which can be an arbitrary function of time), R is the gas constant, E_n and E_g are the respective activation energies, and c_n and c_g are suitable constants.

At time t the radius of an island originated at a previous time $\bar{t}$, is

$$r(t,\bar{t}) = \int_{\bar{t}}^{t} K_g(t')\,\mathrm{d}t'. \tag{3}$$

and the growth rate of its area ($A = \pi r^2$) is

$$\frac{\mathrm{d}A(t,\bar{t})}{\mathrm{d}t} = 2\pi r(t,\bar{t}) K_g(t). \tag{4}$$

Let us denote by $\alpha(t)$ the fraction of the surface F covered by the oxidation islands at time t; $\alpha(t) \leqslant 1$. At time $\bar{t}$, the total uncovered area of the surface on which new islands can nucleate is thus equal to $[1-\alpha(\bar{t})]F$, and the total number of new islands that come into being during an infinitesimal time interval $\mathrm{d}\bar{t}$ is [1]

$$\mathrm{d}n(\bar{t}) = [1-\alpha(\bar{t})] F K_n(\bar{t})\,\mathrm{d}\bar{t}. \tag{5}$$

As the islands grow, they come into mutual contact and slowly merge into a stochastic interconnected network of oxidized areas of complicated geometrical structure, the area of which is difficult to calculate. What can be calculated rather easily instead, is an auxiliary quantity equal to the sum A_T of the areas of all circular islands, assuming that they preserve their circular form indefinitely, as if they grew over each other, covering the whole surface many times over in due time. A_T has no physical meaning, it is introduced solely to simplify mathematical manipulations. It is obtained by multiplying the area of a single island of Eq. (4) by the number of island of the same size as given by Eq. (5), and integrating from the start of the nucleation (oxidation) process, which we put at $t = 0$, i.e.,

$$A_T(t) = \int_0^t A(t,\bar{t})\,\mathrm{d}n(\bar{t}). \tag{6}$$

[1] Unlike in some other processes involving nucleation and growth in which further nucleation is inhibited after an initial distribution of some small entities (nuclei) is established, there is no such inhibition in the surface oxidation studied here. The access to oxygen is the same for all possible nucleation sites on a planar solid surface. As long as a site remains on the uncovered fraction of the surface, the probability that it becomes a new nucleus (i.e., the rate of nucleation) is not influenced but the presence of older nuclei/islands in other parts of the surface. Therefore, nucleation continues as long as $\alpha < 1$.

We can introduce a dimensionless 'surface fraction', $\alpha'(t) = A_T(t)/F$, also for this auxiliary quantity. Eqs. (6) and (5) then give

$$\alpha'(t) = \int_0^t A(t,\bar{t})[1-\alpha(\bar{t})]\,K_n(\bar{t})\,\mathrm{d}\bar{t}. \tag{7}$$

For most cases involving high enough temperatures one gets

$$\lim_{t\to\infty} \alpha'(t) = \infty. \tag{8a}$$

This is true for example for all isothermal cases, because $K_g(t)$ depends on time only through the time dependence of temperature. Only if temperature decreases so fast that $K_g(t)$ goes to zero at least exponentially for large times, can one get a finite value of $\alpha'(\infty)$. On the other hand, the actual fractional surface coverage $\alpha(t)$ can never exceed 1, and in the cases of constant non-zero K_g one has

$$\lim_{t\to\infty} \alpha(t) = 1. \tag{8b}$$

Only for small times, before the first two islands do join, do we have $\alpha'(t) = \alpha(t)$. This implies, that, in the least, the following two relations must be satisfied when $\alpha = 0$, i.e., at $t = 0$:

$$\alpha'(0) = \alpha(0) = 0, \tag{9a}$$

and

$$\frac{\mathrm{d}\alpha'(0)}{\mathrm{d}t} = \frac{\mathrm{d}\alpha(0)}{\mathrm{d}t}. \tag{9b}$$

The simplest relation between $\alpha(t)$ and $\alpha'(t)$ satisfying conditions (8a)–(9b) is

$$\alpha = 1 - \mathrm{e}^{-\alpha'}. \tag{10}$$

According to Ref. [2], this seems to be a generally accepted approximation for the description of the stochastic process of the island merging. Although this approximation seems to be of a somewhat arbitrary nature, it is actually quite reasonable. In Ref. [1] it was found in agreement with a finite element simulation of the process of island oxidation of UO_2. One has to bear in mind that we are only interested in situations with $\alpha \leqslant 0.5$. Namely, for higher values of the surface coverage one cannot obtain useful experimental data to compare this theory with, because $\alpha = 0.5$ roughly corresponds to the onset of spallation. And for $\alpha < 0.5$ there is hardly any approximation involved because in this range α' does not differ much from α. For $\alpha = 0.5$, Eq. (10) still gives for α' only the value of 0.693. Even for nearly fully covered surface, α' goes to infinity rather slowly. Thus for $\alpha = 0.9$ one has $\alpha' = 2.3$, and $\alpha = 0.99$ corresponds to $\alpha' = 4.6$. Eq. (10) simply represents an elegant smoothing of the random network of merging islands for high and experimentally uninteresting values of α, which makes it possible to perform in what follows most of the analysis analytically, while introducing only negligible error for smaller values of α that are of interest here. Nucleation always correctly takes place on and only on that fraction of the surface that is actually uncovered, see Eq. (5).

From Eq. (10) we have

$$\frac{\mathrm{d}\alpha}{\mathrm{d}t} = [1-\alpha]\frac{\mathrm{d}\alpha'}{\mathrm{d}t}, \tag{11}$$

and from Eq. (7)

$$\frac{\mathrm{d}\alpha'(t)}{\mathrm{d}t} = \int_0^t \frac{\mathrm{d}A(t,\bar{t})}{\mathrm{d}t}\,[1-\alpha(\bar{t})]\,K_n(\bar{t})\,\mathrm{d}\bar{t}, \tag{12}$$

where we have used the obvious fact that $A(t,t) = 0$. Substituting this into Eq. (11), and using Eq. (4) gives

$$\frac{\mathrm{d}\alpha(t)}{\mathrm{d}t} = 2\pi K_g(t)\,[1-\alpha(t)] \int_0^t r(t,\bar{t})\,[1-\alpha(\bar{t})]\,K_n(\bar{t})\,\mathrm{d}\bar{t}, \tag{13}$$

which is the sought kinetic equation describing the evolution of the surface coverage for the arbitrary nucleation and growth rates, under the approximation of Eq. (10).

Let us introduce the following two auxiliary functions:

$$f(t) = \int_0^t r(t,\bar{t})K_n(\bar{t})\,[1-\alpha(\bar{t})]\,\mathrm{d}\bar{t} \tag{14a}$$

and

$$g(t) = \int_0^t K_n(\bar{t})\,[1-\alpha(\bar{t})]\,\mathrm{d}\bar{t}. \tag{14b}$$

Then it is easy to verify, that the integro-differential equation (13) is equivalent to the following system of ordinary differential equations of the first order:

$$\frac{\mathrm{d}\alpha(t)}{\mathrm{d}t} = 2\pi K_g(t)\,[1-\alpha(t)]\,f(t), \tag{15a}$$

$$\frac{\mathrm{d}f(t)}{\mathrm{d}t} = K_g(t)g(t), \tag{15b}$$

$$\frac{\mathrm{d}g(t)}{\mathrm{d}t} = K_n(t)\,[1-\alpha(t)], \tag{15c}$$

and

$$\alpha(0) = f(0) = g(0) = 0. \tag{15d}$$

This system can be easily solved numerically using standard methods such as that of Runge–Kutta or the numerical integration capabilities of the recent computer algebra systems (here we used Maple V [3]).

3. Isothermal case

When the temperature is constant in time, both K_g and K_n are also constant in time, and

$$r(t,\bar{t}) = K_g(t-\bar{t}).$$

Eq. (13) then becomes

$$\frac{\mathrm{d}\alpha(t)}{\mathrm{d}t} = 2\pi\kappa[1-\alpha(t)]\int_0^t (t-\bar{t})[1-\alpha(\bar{t})]\,\mathrm{d}\bar{t}, \tag{16}$$

where

$$\kappa = K_g^2 K_n$$

is a 'lumped' rate constant. From Eqs. (1) and (2) one has

$$\kappa(T) = c_\kappa \mathrm{e}^{-E_\kappa/RT}, \tag{17a}$$

where

$$c_\kappa = c_n c_g^2, \tag{17b}$$

and

$$E_\kappa = E_n + 2E_g. \tag{17c}$$

One can introduce dimensionless time,

$$\tau = t\sqrt[3]{\pi\kappa}, \tag{18}$$

and go back to α' in Eq. (16) to obtain

$$\frac{\mathrm{d}\alpha'(\tau)}{\mathrm{d}\tau} = 2\int_0^\tau (\tau-\bar{\tau})\,\mathrm{e}^{-\alpha'(\bar{\tau})}\,\mathrm{d}\bar{\tau}.$$

Differentiating now this equation twice with respect to τ, one gets

$$\frac{\mathrm{d}^3\alpha'(\tau)}{\mathrm{d}\tau^3} = 2\mathrm{e}^{-\alpha'(\tau)}. \tag{19}$$

Note that in the isothermal case, transformation (18) produces a parameter-less kinetic equation. It suffices to solve it once for ever, and then simply scale the time according to Eq. (18) to obtain solutions for different values of κ.

Introducing auxiliary functions $\phi(\tau)$ and $\gamma(\tau)$, one can convert Eq. (19) into a system of ordinary differential equations:

$$\frac{\mathrm{d}\alpha'(\tau)}{\mathrm{d}\tau} = 2\phi(\tau), \quad \frac{\mathrm{d}\phi(\tau)}{\mathrm{d}\tau} = \gamma(\tau), \quad \text{and} \quad \frac{\mathrm{d}\gamma(\tau)}{\mathrm{d}\tau} = \mathrm{e}^{-\alpha'(\tau)}.$$

Returning to α with the help of Eqs. (10) and (11) finally gives

$$\frac{\mathrm{d}\alpha(\tau)}{\mathrm{d}\tau} = 2[1-\alpha(\tau)]\phi(\tau), \tag{20a}$$

$$\frac{\mathrm{d}\phi(\tau)}{\mathrm{d}\tau} = \gamma(\tau), \tag{20b}$$

$$\frac{\mathrm{d}\gamma(\tau)}{\mathrm{d}\tau} = 1-\alpha(\tau), \tag{20c}$$

and

$$\alpha(0) = \phi(0) = \gamma(0) = 0. \tag{20d}$$

This is a variation of the system (15a)–(15d) and it could be obtained directly from it using transformation (18), and the following definitions:

$$\phi(\tau) = \frac{\pi K_g}{\sqrt[3]{\pi\kappa}} f(t) \quad \text{and} \quad \gamma(\tau) = \pi\left(\frac{K_g}{\sqrt[3]{\pi\kappa}}\right)^2 g(t).$$

The reason why we went via Eq. (19) is that it can be used as the easiest starting point to derive a power-series solution for the isothermal case. Because of the initial conditions (20d), which are equivalent to

$$\alpha'(0) = \frac{\mathrm{d}\alpha'(0)}{\mathrm{d}\tau} = \frac{\mathrm{d}^2\alpha'(0)}{\mathrm{d}\tau^2} = 0,$$

and the form of Eq. (19), the Taylor series for $\alpha'(\tau)$ has only terms with powers that are multiples of three:

$$\alpha'(\tau) = \sum_{j=1}^{\infty} a_j \tau^{3j}. \tag{21}$$

Substituting this expansion into Eq. (19) gives for the first few coefficients a_j the following values:

$$a_1 = \frac{1}{3}, \quad a_2 = -\frac{1}{180}, \quad a_3 = \frac{11}{45\,360},$$
$$a_4 = -\frac{5}{399\,168} \quad \text{and} \quad a_5 = \frac{9299}{13\,621\,608\,000}.$$

Apparently, the absolute value of a_j goes to zero very fast as j increases and so truncating Taylor series (21) after just a few terms can be expected to give a very good approximation for a large range of τ values. Substituting Taylor series (21) truncated after k terms into Eq. (10) gives the following approximation for $\alpha(\tau)$:

$$\alpha(\tau) = 1 - \exp\left[-\sum_{j=1}^{k} a_j \tau^{3j}\right]. \tag{22}$$

As for any truncated Taylor series, increasing the number of terms, k, increases the range of small positive τ values over which the truncated series is practically identical with the exact solution obtained by solving numerically Eqs. (20a)–(20d). In addition to that, in this particular case all even terms a_{2i} are negative, and thus truncated series (22) obviously diverges to the unphysical value of $-\infty$ as $\tau \to \infty$ for all even k, whereas it goes to the correct limit of 1 for all odd k. Therefore, one should use only the odd-term terminated truncations as

they give a good approximation of $\alpha(\tau)$ for all values of τ. Such approximations differ from the exact solution only in a range of medium values of τ. This range will become narrower as the (odd) number of terms, k, is increased. Fig. 1 compares the exact solution (solid line) with the approximate solution for several values of k. It indicates that the difference between the exact and approximate solutions is rather small even for $k = 1$ when it is significant only for $\tau \in (1, 3)$ and never larger than about 0.021. And $k = 3$ already gives an approximate solution that is almost identical with the exact one for all practical purposes—it differs noticeably from the exact solution only for $\tau \in (1.8, 2.7)$ with the maximum difference being about 0.0047. Note that all the approximate solutions for odd k seem to be larger than the exact one, whereas those for the even k are less than the exact one (cf. Fig. 1(b)). And the solution for $k = 4$ starts to diverge to $-\infty$ sooner than that for $k = 2$.

Comparing this theoretical solution of Eq. (16) (or (19)) with the evolution of the surface coverage observed in a series of isothermal experiments, it is possible to determine the temperature dependence of the lumped rate constant κ of Eqs. (17a)–(17c). Specifically, for the formation of U_3O_8 on the surface of unirradiated UO_2,

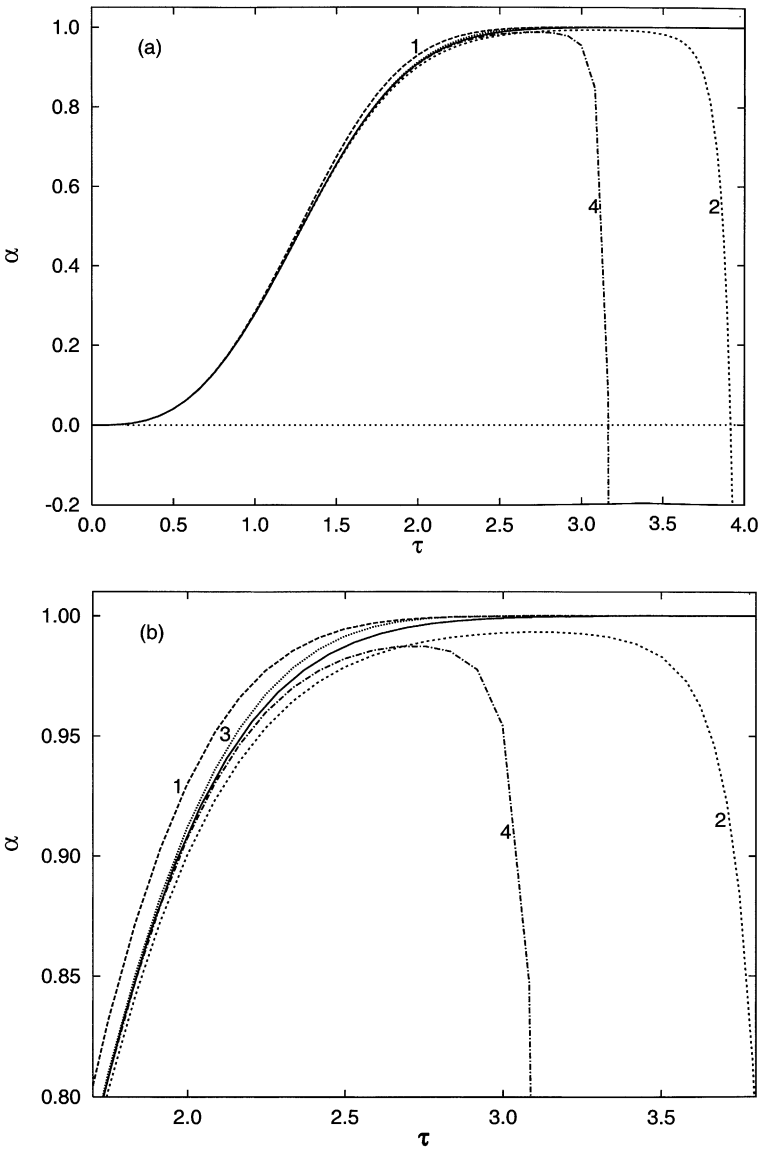

Fig. 1. Comparison of the exact solution (solid line) of the isothermal Eqs. (20a)–(20d) with the truncated power-series approximation for several values of k (as indicated). (a) Full range of α. (b) The large-α portion of (a) magnified.

comparing the experimental results with the $k = 1$ approximation,

$$\alpha(t) = 1 - e^{-\pi\kappa t^3/3} \tag{23}$$

(cf. Eqs. (18) and (22)), it was determined in Ref. [1] that

$$c_\kappa = e^{86.165}\,h^{-3} = e^{113.401}\,a^{-3} \quad \text{and}$$
$$E_\kappa = 52\,808.0\,R. \tag{24}$$

These are the values that will be used in all numerical examples (and in all figures) in what follows. They represent the maximum that can be determined from isothermal experiments only. To determine the two constituent components of κ, one has to design suitable non-isothermal experiments, as will be discussed in the next section. For various spent fuels the value of E_κ may be different from that of Eq. (24). Then the whole analysis of the next section has to be repeated with the correct data for a given sample.

4. Non-isothermal case – suggestions for experimental studies

First note that Eq. (13) is invariant to simultaneously replacing c_n by $c_n C^2$ and c_g by c_g/C, where C is an arbitrary constant. Therefore, the value of fraction covered (oxidized), $\alpha(t)$, remains unchanged if constants c_n and c_g of Eqs. (1) and (2) are varied such that the product $c_n c_g^2$ (c_κ of Eq. (17b)) remains constant. In other words, a C^2-fold increase in the nucleation rate can be compensated by a simultaneous C-fold decrease in the growth rate without any effect on the time dependence of the surface coverage α. Measuring only the surface coverage, whatever the time dependence of the temperature, one cannot determine the individual values of two constant c_n and c_g, only their product c_κ.

What always varies with c_n and c_g is the size and number of individual oxidation islands. Therefore, to determine directly the values of c_n and c_g, one would have to measure for example the growth rate of the diameters of a set of well defined islands. It would suffice to do that at a single value of constant temperature, so as to determine the absolute value of K_g at that temperature. Using then the isothermal results such as those of Eq. (24), and the individual values of the activation energies E_g and E_n determined from non-isothermal experiments such as the ones suggested in what follows, one would be able to determine also the values of c_n and c_g.

It is impossible to find even an approximate analytical solution (such as a truncated power-series expansion) of Eq. (13) or of the equivalent system (15a)–(15d) for the general case of arbitrary time dependence of the temperature. This could be done only if temperature is an analytical function of time, and even then it might be feasible only in some special cases, such as when the inverse temperature is a linear function of time.

For the purpose of determining the values of E_g and E_n by comparing experimental data to theoretical results, one has to solve the system of Eqs. (15a)–(15d) numerically for a whole series of values of E_g and E_n satisfying constraint (17c) with E_κ given by Eq. (24), and using the same time dependence of temperature as in the experiments. Then those values of E_g and E_n that give the best agreement with the experiments are the result of our measurement.

4.1. Long-term hypothetical temperature variation

At first, let us illustrate how big the effect of variation of (uncertainty in) the activation energies of K_n and K_g may be in a 'real-life' situation. Let us determine the time dependence of the oxidized fraction α of U_3O_8 on the surface of unirradiated UO_2 for the temperature profile of Fig. 2 which represents a plausible scenario that may be encountered by used fuel in a dry air storage facility [4].

Three special cases of possible temperature dependence of K_n and K_g within the constraints set by Eqs. (17c) and (24) are discussed first:

(1) $E_g = E_n = E_\kappa/3$.
(2) $E_g = 0$, $E_n = E_\kappa$.
(3) $E_n = 0$, $E_g = E_\kappa/2$.

Case (1) is a 'median' case in the sense that the activation energies of both rate constants are the same, whereas the other two cases represent the extreme cases when one of the two rate constants does not depend on temperature

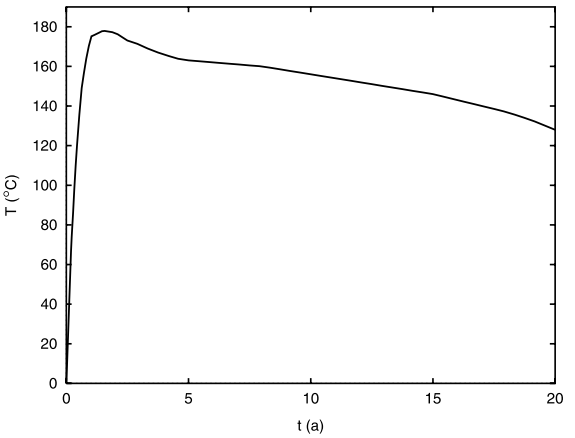

Fig. 2. An expected variation of the surface temperature of the used nuclear fuel emplaced for 20 years in a dry-air-storage facility.

(and thus on time) at all. The time dependence of α corresponding to these three cases is presented in Fig. 3. One can see that the time dependence of α differs significantly for these three cases. In case (2), the surface is covered completely in about 7 years, whereas in the other two cases the growth of α slows down almost to a halt: at 20 a, α increases at a rate of mere 0.002 a^{-1} and 0.0003 a^{-1} for cases (1) and (3), respectively.

Results of these calculations for other intermediate values of E_g and E_n are presented in Fig. 4, which shows the surface coverage after 1.5, 2.5, 10 and 20 years from the start of the oxidation process as a function of the

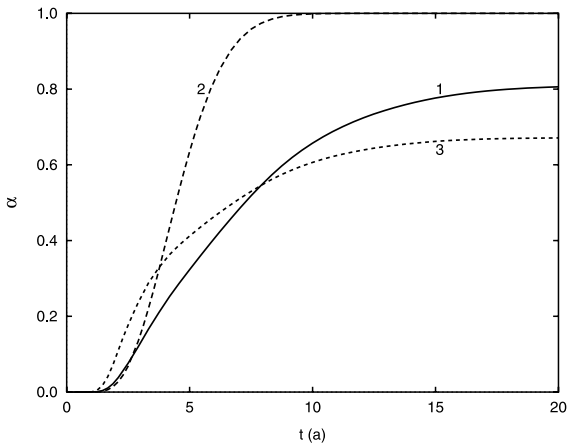

Fig. 3. Time dependence of the surface coverage α for temperature profile of Fig. 2 for three different possible decompositions of E_κ: (1) $E_g = E_n = E_\kappa/3$ (solid line); (2) $E_g = 0$ and $E_n = E_\kappa$ (dashed line); and (3) $E_g = E_\kappa/2$ and $E_n = 0$ (dotted line).

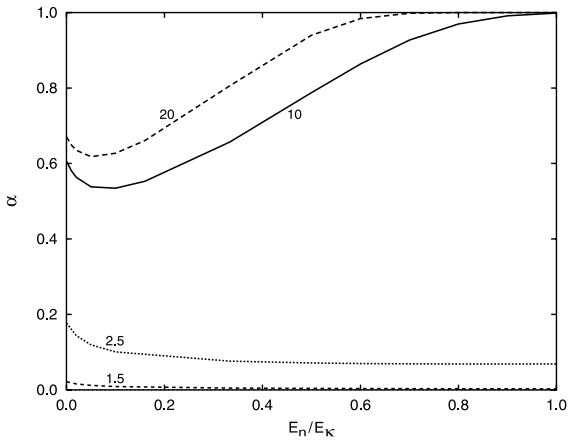

Fig. 4. The surface coverage α for temperature profile of Fig. 2 after 1.5, 2.5, 10 and 20 years (as indicated) shown as a function of the nucleation rate activation energy (expressed as a fraction of the lumped rate activation energy E_κ of Eq. (24)).

nucleation rate activation energy expressed as a fraction of the lumped activation energy E_κ (and the growth rate activation energy is then given by Eq. (17c)). It was verified that the integration procedure (using 15 digit precision) was very stable and the results were independent of the choice of c_n and c_g (bound by the constraint (17b)).

One can see that the actual values of E_n and E_g have significant effect on the relative rate of the surface coverage in different time intervals. For small E_n (and thus large E_g) α increases very rapidly initially but its increase is slowed down at larger times. For large E_n the opposite is true.

In the next subsection it will be shown how carefully designed accelerated experiments at higher temperatures could be used to determine the values of E_n and E_g needed for the exact prediction of the long-term behavior of various oxidizing UO_2 surfaces (such as those of used fuel placed in dry air storage facilities).

4.2. Short-term experiments with linear variation of temperature

To achieve the total coverage of the surface within a month from the beginning of the experiment, one has to increase the maximum temperature to somewhere between 250 and 300 °C. Examples of the time dependence of the surface coverage α obtained at such elevated temperatures for linear (increasing or decreasing, or first increasing and then decreasing) temperature variation over a 30 days period are presented in Figs. 5–8. Again, the lumped rate values of Eq. (24) were used.

We first simulated a rather slow monotonic increase of temperature from 100 to 300 °C in 30 days. The oxidation started to speed up rapidly only when the temperature of 250 °C, achieved after 20 days, was being approached. All the curves for different E_n (E_g) values were rather close together. Nevertheless, if such an experiment could be stopped after 21 days (samples had to be cooled down instantaneously to stop further oxidation), it would give the largest resolution, of all the temperature scenarios discussed here, in the range $0 < E_n/E_\kappa \lesssim 0.9$: the spread of the α values in this range is almost 0.8. However, there is practically no resolution when E_n approaches E_κ (E_g goes to 0). If instant cooling is impossible, simulations for modified temperature profiles including gradual cooling (for example a linear decrease of temperature after 21 or 22 days to 100 °C over a period of one day) show that the resolution would decrease everywhere.

It thus seems that there is no point in increasing the temperature above about 260 °C. Fig. 5 shows what happens if temperature is slowly monotonically increased only in the range of onset of fast oxidation, between 200 and 260 °C in 30 days. One can see that the spread of the curves for different E_n values is increased

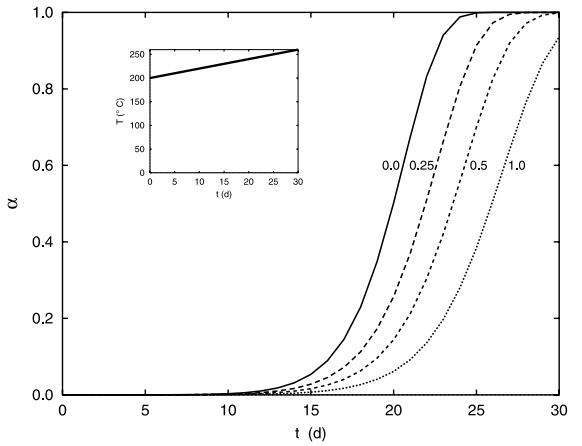

Fig. 5. Time dependence of the surface coverage α for linear temperature increase from 200 to 260 °C over 30 days (see the inset). Different curves correspond to different values of E_n/E_κ as indicated.

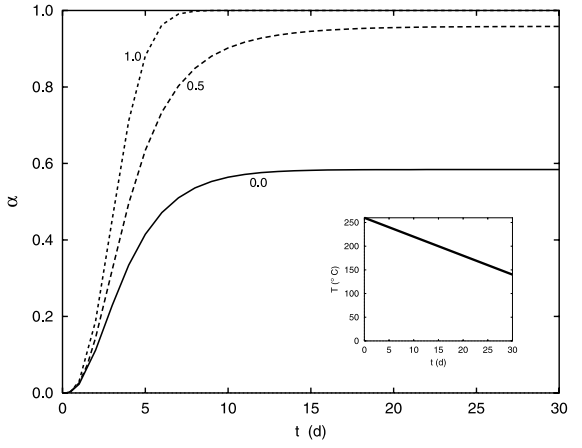

Fig. 6. Time dependence of the surface coverage α for linear temperature decrease from 260 to 140 °C over 30 days (see the inset). Different curves correspond to different values of E_n/E_κ as indicated.

but the results are otherwise not significantly different from those for the 100–300 °C temperature ramp. Fig. 6 then shows the results for a monotonic linear decrease of temperature from 260 to 140 °C (assuming instantaneous heating to 260 °C at the beginning of the experiment). Note that the order of curves is reversed with the reversal of the temperature variation: When the temperature is increasing, the fastest covering of the surface occurs when $E_n = 0$ (no dependence of the nucleation rate on temperature and the strongest dependence of the growth rate on temperature), whereas when the temperature is decreasing, the fastest covering occurs for $E_n = E_\kappa$ (no dependence of the growth rate on temperature and the strongest dependence of the nucleation rate). In both cases, the resolution for $E_n \to E_\kappa$ remains poor.

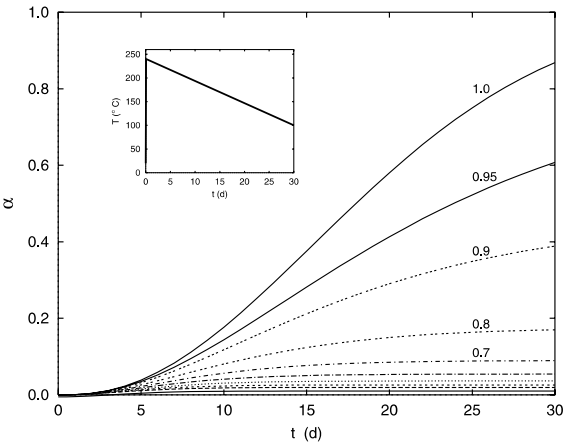

Fig. 7. Time dependence of the surface coverage α for piecewise linear temperature variation starting with a fast linear increase from 20 to 240 °C in 2 h followed by a slow linear decrease to 100 °C in 718 h (total duration is again 30 days; see the inset). Different curves correspond to different values of E_n/E_κ as indicated. The five lowest curves correspond to $E_n/E_\kappa = 0.2$, 0.3, 0.4, 0.5 and 0.6.

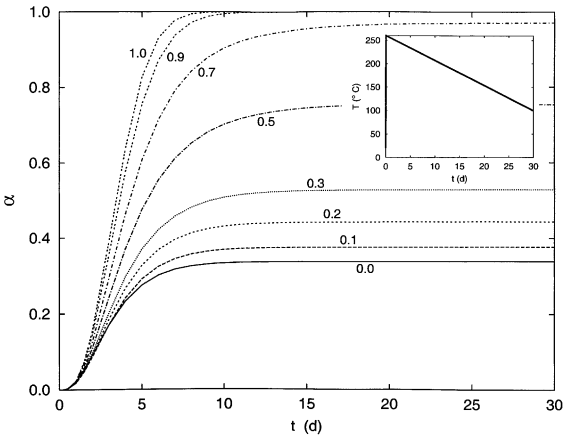

Fig. 8. Time dependence of the surface coverage α for piecewise linear temperature variation starting with a fast linear increase from 20 to 260 °C in 2 h followed by a slow linear decrease to 100 °C in 718 h (total duration is again 30 days; see the inset). Different curves correspond to different values of E_n/E_κ as indicated.

Finally Figs. 7 and 8 represent more realistic experimental scenarios – they consider both the heating of the sample followed by gradual cooling. When the heating phase is much shorter than the cooling phase (as in the scenarios chosen here), the curves for different E_n are still

ordered monotonically with increasing E_n as for the instantaneous heating of Fig. 6. When the duration of both phases is comparable, the monotonic ordering of the curves is lost as in Fig. 3.

One can see that the α curves are quite sensitive to relatively small changes in the temperature scenarios. By slightly changing the peak temperature, one can move the highest resolution 'window' (the region of the E_n/E_κ ratio where the separation of the curves is the largest). It would probably be necessary to perform several simultaneous experiments on identical samples to cover the whole range of possible E_n/E_κ ratios. One limitation that has to be taken into account is that the temperature scenarios must be chosen so that the surface coverage α does not exceed the value of about 0.5. This corresponds to the onset of spallation, above which the oxidation is not limited to a smooth surface any more. The scenarios of Figs. 7 and 8 and two additional intermediate scenarios occurring in Fig. 9 were designed with this fact in mind.

Fig. 9 indicates how the results of four simultaneous experiments on identical samples using different temperature scenarios could be used to determine experimentally the ratio E_n/E_κ. If one marks on each curve the point corresponding to the final value of α observed in the respective experiments, all four points should lie on a single horizontal line, the intersection of which with the vertical axis determines the value of E_n/E_κ for the samples used. How well are the four points aligned horizontally is the measure of the experimental accuracy.

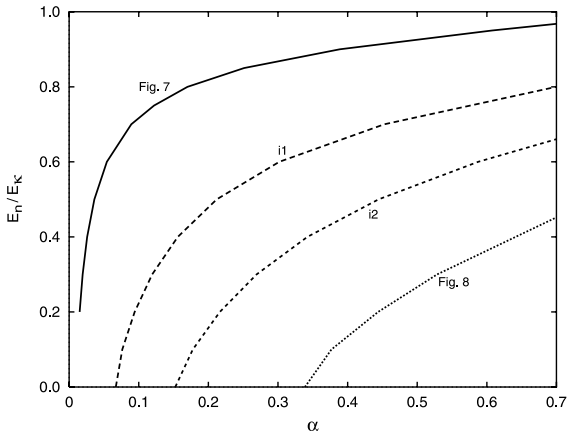

Fig. 9. Comparison of the final surface coverage α for the 30-day temperature scenarios of Figs. 7 and 8 and two intermediate scenarios i1 and i2, as a function of the ratio E_n/E_κ. The intermediate scenarios are: i1 – a fast linear increase from 20 to 250 °C in 2 h followed by a slow linear decrease to 100 °C in 718 h; i2 – fast linear increase from 20 to 255 °C in 1 h followed by a slow linear decrease to 100 °C in 719 h. The final values of α obtained in four simultaneous experiments on identical samples subjected to these temperature scenarios must lie on a horizontal line the position of which gives the value of E_n/E_κ for the given samples.

The examples discussed here hopefully illustrate well enough that adjusting suitably the maximum temperature and the duration of the heating and the cooling phases can increase the resolution in a particular range of the E_n values. It is relatively easy to solve numerically the system of Eqs. (15a)–(15d) for any temperature scenario. Therefore, any number of simulations of this type can be carried out in conjunction with an actual experiment, for the actual temperature variation used in the experiment, which can be an arbitrary function of time. The value of E_n/E_κ can be progressively refined by designing optimized temperature scenarios with the highest resolution window in that region of E_n/E_κ values in which E_n/E_κ was found in the previous lower-accuracy experiments.

5. Summary and conclusions

The theory of the surface coverage in the island-like oxidation of certain solid surfaces was presented, and applied to the case of unirradiated UO_2. Exactly the same procedure could be used for used fuel surface. The previous paper [1] on the isothermal case was complemented by the observation that only the odd-term-terminated truncated Taylor-series approximations for the isothermal time dependence of the surface coverage should be used.

However, the main new contribution of this paper is numerical exploration of various non-isothermal scenarios—a plausible long-term real-life nuclear-used-fuel dry-air-storage scenario, and various accelerated linear experimental scenarios at elevated temperatures. Suggestions were presented on how to determine separately the activation energies of the nucleation rate and the growth rate constants using a series of experiments on identical samples with slightly different temperature scenarios. Any such experimental studies should be accompanied by numerical simulations of the type presented in Section 4.2 for exactly the same temperature scenarios as the ones used in the experiments. By fine tunning the temperature scenarios, one can increase the resolution of different ranges of the values of the activation energies. In this way, one could successively increase the accuracy of measurements by moving the center of the high-resolution window to the previous estimate of the activation energy (of nucleation).

Note added in proof

In the case of U_3O_8, the circular islands may be just a conceptual model that is useful in interpreting

experimental data in a standardized, quantitative way. Experimental recommendations of this paper may be useful for further verification of this model.

Acknowledgements

The author is grateful to Rod McEachern for stimulating discussions, and appreciates critical review of the manuscript by Dennis LeNeveu.

References

[1] R.J. McEachern, J.W. Choi, M. Kolář, W. Long, P. Taylor, D.D. Wood, J. Nucl. Mater. 249 (1997) 58.
[2] F.C. Tompkins, in: N.B. Hannay (Ed.), Treatise on Solid State Chemistry, Vol. 4, Reactivity of Solids, Plenum, New York, 1976.
[3] M.B. Monagan, K.O. Geddes, K.M. Heal, G. Labahn, S.M. Vorkoetter, Maple V, Waterloo Maple. http://www.maplesoft.com.
[4] P. Taylor, R.J. McEachern, unpublished.